Applications of Automation Methods for Nonlinear Fracture Test Analysis

Phillip A. Allen[1] and Douglas N. Wells[2]

Abstract

As fracture mechanics material testing evolves, the governing test standards continue to be refined to better reflect the latest understanding of the physics of the fracture processes involved. The traditional format of ASTM fracture testing standards, utilizing equations expressed directly in the text of the standard to assess the experimental result, is self-limiting in the complexity that can be reasonably captured. The use of automated analysis techniques to draw upon a rich, detailed solution database for assessing fracture mechanics tests provides a foundation for a new approach to testing standards that enables routine users to obtain highly reliable assessments of tests involving complex, non-linear fracture behavior. Herein, the case for automating the analysis of tests of surface cracks in tension in the elastic-plastic regime is utilized as an example of how such a database can be generated and implemented for use in the ASTM standards framework. The presented approach forms a bridge between the equation-based fracture testing standards of today and the next generation of standards solving complex problems through analysis automation.

[1]Corresponding Author, Materials and Process Laboratory, NASA Marshall Space Flight Center, MSFC AL, 35812
[2]Materials and Process Laboratory, NASA Marshall Space Flight Center, MSFC AL, 35812

Introduction

Mechanical test standards are intended to enable users to test materials in a controlled and consistent manner to evaluate a material property repeatably from one laboratory to another. In the realm of fracture toughness test standards, the test methods take a complicated physical process, the fracture of materials, and distill it through fracture mechanics principles to single material property–the fracture toughness. This is not a trivial task due to the complex nature of the fracture process and the wide range of applicable material types with their various associated fracture mechanisms. As the fracture mechanics community develops further understanding of the detailed mechanics of fracture processes, the authors of fracture mechanics testing standards struggle with two, sometimes opposing, goals: 1) creating test standards that accurately reflect the physics of the problem and consistently produce the "most correct" answers, and 2) creating test standards that are not overly complex and burdensome for the user. Ideally both of these goals would be achieved: fracture mechanics test standards could capture and explain the physics of the problem, while not being arduous to use or require particularly unique expertise to execute reliably.

All of the current ASTM fracture testing standards such as E399 [1] and E1820 [2] take the three-dimensional (3-D) reality of the fracture test and, through the use of various assumptions, simplify the problem to a two-dimensional planar form to report an average fracture toughness representing the entire crack front. In general, the simplifications required to reduce all the relations needed to evaluate the fracture mechanics test into a tractable form for conveyance in print limits the ability to accommodate heightened complexity, such as multiple forms of non-linearity. For example, E1820 addresses material plasticity through the use of η_{pl} factors to calculate the plastic portion of the J-integral, but does not address the through-thickness

nonlinear variation of the crack front *J*-integral values. These simplifying assumptions are not inappropriate; in fact, they allow standards to provide manageable equations for the calculation of toughness values that are reasonable engineering approximations of the actual 3-D problem. However, the current framework of test standards requiring this level of distillation of the solution clearly limits the scope of test complexity that can be accommodated.

As more complicated fracture toughness tests are considered for standardization, it may not be practical or desirable to reduce the fracture toughness test analysis down to a simple equation form. Consider the difficulties that arise in assessing laboratory fracture toughness tests with surface cracks. (see Figure 1) In these tests, due to practical specimen size limitations, the material fracture toughness is commonly not reached until well beyond the linear-elastic fracture mechanics (LEFM) limit. In addition the surface crack toughness test is highly three-dimensional with a crack driving force that varies nonlinearly along the crack perimeter. The advance of surface crack fracture testing is hindered significantly by the lack of a readily available set of solutions to correlate the applied force and observed crack mouth opening displacement (*CMOD*) in a surface crack experiment to an evaluation of the elastic-plastic *J*-integral or deformation state of a test specimen at fracture. Currently, the only practical way to fully analyze such a test is through the use of elastic-plastic finite element analysis. A convenient and practical set of elastic-plastic surface crack solutions could help mitigate many of these obstacles; however, to date, it has proven impractical to reduce the 3-D elastic-plastic surface crack solution to a set of equations suitable for inclusion in a testing standard. Herein, the authors utilize the surface crack example to illustrate the use of analysis automation to offer a solution to this dilemma and argue for a new generation of test standards based on more advanced, automated methods of test analysis.

In the years prior to the advent of routine finite element based fracture mechanics analysis, many researchers provided alternative and robust engineering solutions to the elastic-plastic surface crack problem, though subject to many practical limitations. An excellent summary of the development of elastic-plastic *J*-integral solutions up to the year 1999 is given by McClung *et al*. [3]. Apart from FEA, the commonly used methods for calculating elastic-plastic *J*-integral solutions usually follow one of two basic techniques [4]: the Electric Power Research Institute (EPRI) approach [5-7] or the reference stress method (RSM) [8]. The EPRI and RSM techniques have found wide application in analysis of structures, but have limited application in the detailed assessment of surface crack laboratory tests. Understanding the crack tip conditions at the point the fracture toughness is reached in an experimental surface crack test requires knowledge of the specimen geometry, the applied force, *P*, the resulting *CMOD* response, the elastic-plastic flow properties of the material, and a corresponding solution for the *J*-integral versus ϕ relationship as it evolves with increasing specimen deformation. The current RSM and EPRI solutions for surface cracks do not provide the user with the full *P* versus *CMOD* trace which serves as the most fundamental connection between experiment and analysis. The measured *CMOD* value provides the most robust predictor of the *J*-integral values at the crack tip [4,9]. In addition, most of the current RSM and EPRI solutions only provide results at a limited number of crack perimeter ϕ locations and have *J* versus ϕ relationships that are based on either linear-elastic solutions (RSM) or fully plastic solutions (EPRI), neither of which capture the changes in the *J* versus ϕ distribution and maximum *J*-integral location as elastic-plastic deformation increases.

Working within an ASTM task group, the authors have developed a new surface crack testing standard, still in the approval balloting process as of this writing. The current version of the test standard provides mandatory equations (Newman-Raju Equations [10,11]) for solutions

within the linear-elastic regime, but requires the use of an independent FEA for test evaluations in the elastic-plastic regime. Once released, it will be the first ASTM fracture mechanics testing standard allowing a test result to be obtained from a method other than standardized equations codified in print. Though both flexible and enabling in scope, this method for evaluating an elastic-plastic surface crack test result requires a unique and time-consuming FEA for each test. While elastic-plastic fracture mechanics (EPFM) assessment of surface cracks has become significantly more accessible through improved finite element interfaces such as FEACrack™ [12] or ABAQUS® CAE [13], the cost of such assessments in analysis time, code licensing, and requisite user expertise remain, unfortunately, a significant impediment to common use.

With the advent of today's computing power and inexpensive data storage, an alternative method for providing a solution to a complex mechanics problem is to pre-solve the solution space and provide a method for interpolating to the correct solution through automated analytical methods. A fracture mechanics test, even a complicated one such as the elastic-plastic surface crack test, is a bounded problem based on the practical limitations of specimen geometries, engineering material properties, and defined loading conditions. In addition, an automated method for interpolating between pre-solved solutions eliminates the need for the user to interpret and program the equations from the standard and, thereby, should result in a more reliably "standard" answer for the test. The methodology of pre-solving the problem and interpolating to an answer allows the common user to get a high fidelity solution that captures the latest understanding in the physics of the problem without the restrictions and distillations associated with equations. This methodology directly utilizes the 3-D FEA solutions, avoiding the need to fit numerous nonlinear equations to the solution space and the loss of fidelity that usually accompanies such multi-dimensional fits. This approach forms a bridge between the

equation-based ASTM fracture testing standards of today and the next generation of standards for complex problems.

As an example of a pre-solved solution methodology, this paper briefly describes a simple and robust method developed by the authors for analyzing surface crack tension tests based on an array of 600, 3-D nonlinear finite element models for surface cracks in flat plates under tension loading. The solution space covers a wide range of crack geometric parameters and material properties. The solution of this large array of nonlinear models was made practical by computer routines that automate the process of building the finite element models, running the nonlinear analyses, post-processing model results, and compiling and organizing the solution results into multi-dimensional arrays. The authors have developed a methodology for interpolating between the geometric and material property variables that allows the user to estimate the *J*-integral solution around the surface crack perimeter (ϕ) as a function of loading condition from the linear-elastic regime continuously through the fully elastic-plastic regime. In addition to the *J*-integral solution, the complete force versus *CMOD* record is estimated to provide a direct anchor to the experimental result. The user of this interpolated solution space need only know the crack and plate geometry and the basic material flow properties to reliably evaluate the full surface crack *J*-integral and force versus *CMOD* solution; thus, a solution can be obtained very rapidly by users without elastic-plastic fracture mechanics finite element modeling experience. The solution method has been incorporated into a computer program with a graphical user interface (GUI) to allow easy access to the solution space.

Surface Crack Solution Procedures

The process of building the new space of surface crack solutions was logistically intense. Though computationally each part of the process followed mostly well established paths, combining those parts effectively into a functional whole required planning at every level. This section provides a brief summary of the solution space and methods. Details of the computational procedures and solution verifications are given in NASA/TP-2013-217480 [14]. The logistics of building, executing, and then assembling the solution space was made practical only through automation.

Solution Space

The solution space for this array of models is four-dimensional. Two dimensions are used to describe surface crack geometric variation, and two dimensions are used to describe material property variation. The material and geometric spaces were carefully crafted to provide sufficient coverage for most common engineering problems without becoming so large as to be intractable. The following sections summarize the choices and reasoning for the material and geometric dimensions of the solution space.

Material Space - Using a linear then power law (LPPL) representation of the stress-strain response defined by

$$\frac{\varepsilon}{\varepsilon_{ys}} = \frac{\sigma}{\sigma_{ys}} \quad \varepsilon \le \varepsilon_{ys}; \qquad \frac{\varepsilon}{\varepsilon_{ys}} = \left(\frac{\sigma}{\sigma_{ys}}\right)^{n} \quad \varepsilon > \varepsilon_{ys}, \tag{1}$$

the material response can be fully defined by just 3 parameters: σ_{ys}, ε_{ys} or E, and n, where σ_{ys} is a representative a yield stress, and ε_{ys} a corresponding yield strain defined by $\varepsilon_{ys} = \sigma_{ys}/E$, with the elastic modulus, E, and n is the strain hardening exponent. If the yield strength is normalized to unity for all materials ($\sigma_{ys} = 1$), then only ε_{ys} and n are required to define the shape of the

stress-strain curve throughout the space. For convenience of eliminating small fractional numbers, the reciprocal of the yield strain is commonly used, E/σ_{ys}.

Figure 2 illustrates the material space for the study described in terms of the six E/σ_{ys} and five n values resulting in thirty different material combinations. In all cases, $\sigma_{ys} = 1$ and Poisson's ratio, $\nu = 0.30$. The names of several common engineering materials are overlaid on the material matrix in Figure 2 to illustrate how some common materials are represented in the material matrix. The low E/σ_{ys} values of 100 to 200 are materials capable of high values of elastic strain, thus they have low elastic modulus and relatively high yield strength, such as many high performance titanium and aluminum alloys. The opposite end of the E/σ_{ys} space with values of $E/\sigma_{ys} = 1000$ have very little elastic strain capability due to high elastic modulus and low yield strength. Austenitic stainless steels are a common example of this material class.

The other dimension of the material space is the strain hardening exponent, n. The values of n range from 3 to 20, spanning the hardening characteristics of most all structural metals from very high strain hardening ($n = 3$) to almost elastic-perfectly plastic behavior ($n = 20$). The specific values of n for this study were chosen to uniformly divide the strain hardening response in the stress versus plastic strain space.

Geometric Space - Figure 3 illustrates the geometric solution space for this study as sketches of cross-sections through the crack plane arranged in terms of crack depth-to-thickness ratio (a/B) and crack depth-to-half-length ratio (a/c) with $0.2 \le a/c \le 1.0$ and $0.2 \le a/B \le 0.8$ for a total of 20 different geometries. For each a/B and a/c combination in Figure 3, the smaller, upper illustration is a sketch of the crack plane cross-section drawn in proportion to the other geometries. (The illustrations for $a/c = 0.2$, $a/B = 0.6$ and $a/c = 0.2$, $a/B = 0.8$ are half-symmetry

drawings to allow space for the proportional sketches.) These sketches allow the reader to visualize the difference in overall cross-section size for each geometry. For each a/B and a/c combination in Figure 3, the lower illustration is a close up view of the crack plane cross-section with the thickness held constant for all geometries. The close-up sketches better illustrate the semi-elliptical crack shape in relation to the specimen thickness. For all geometries, $B = 1$ and $L/W = 2$. Figure 3 lists the $2c$, W, and L values for all the geometries. The plate widths were set equal to the greater of $W = 5 * 2c$ or $W = 5 * B$ to minimize width effects on the J-integral solutions and to ensure that the plates maintained a "plate like" width-to-thickness aspect ratio for small cracks. Utilizing these minimum width criteria precludes the need to include the $W/2c$ ratio as a third variable in the geometric space [14].

Finite Element Models

A total of 600 nonlinear finite element analyses were required to perform the analysis of the 30 material and 20 geometric combinations. All of the finite element models (FEMs) were created using the commercial finite element mesh creation and post-processing tool FEACrack [12], and the finite element analyses were performed using the freely available research code WARP3D version 16.3.1 [15]. All of the surface cracked plates were modeled with 3-D quarter-symmetric FEMs using 20-node reduced integration isoparametric elements (element type *q3disop* in WARP3D). For each model geometry, Figure 3 lists the total number of nodes and elements as well as the number of nodes in the ϕ direction along the crack perimeter. Uniform axial displacements were applied to all of the nodes on the top surface of the plate to apply tension, and the FEMs were loaded with 20 to 30 even load steps with an average of 2-5 Newton iterations for convergence within each step to a tight tolerance on residual nodal forces.

Computational Automation Methods

Handling this large array of nonlinear models was made practical by computer routines that automate the process of building the finite element models, running the nonlinear analyses, post-processing model results, and organizing the solution results into multi-dimensional arrays. Computer routines were written in Matlab to create the file storage directory structure and serve as the overall controller for the model building, execution, and post-processing procedure.

The FEMs were built using FEACrack in batch control mode on a Windows XP computer with Matlab scripts automating FEACrack runs to produce fully defined WARP3D models throughout the defined solution space. For efficient parallel processing analysis, the WARP3D models were solved using a Linux-based server. Once the finite element analyses were complete, a compact set of WARP3D packet result files were returned to the Windows XP computer for post-processing in batch mode with FEACrack, resulting in a set of 600 text-based result files containing all the pertinent model result data. A set of Matlab scripts then consolidated the full data set into arrays of *J*-integral versus ϕ values, far field stresses, and *CMOD* values in an easily indexed data structure.

Interpolation Methodology

Normalization Scheme - To derive useful results from the solution space, interpolation within the geometry and material dimensions is necessary, but scaling of the solutions with respect to geometry and material is also required. The solution space was normalized to a dimensionless state to simplify scaling. There are three primary results in the solution set that need to be normalized: *J*, *CMOD*, and far-field stress, σ. By dimensional analysis it is clear that the *J*-Integral is conveniently normalized by a product of stress and length, therefore the normalized *J*-integral value, J_n, can be written as

$$J_n = \frac{J}{\sigma_{ys} B} \ . \tag{2}$$

The yield stress and plate thickness are particularly convenient normalizing factors because, as discussed previously, both σ_{ys} and B were defined to have unit value in the model space. Thus, the J-integral result from the analysis does not change when normalized. The same follows for the *CMOD* and far-field stress results where

$$CMOD_n = \frac{CMOD}{B} \ , \tag{3}$$

and the normalized far field stress, σ_n, is

$$\sigma_n = \frac{\sigma}{\sigma_{ys}} \ . \tag{4}$$

Solution Space Interpolation - Interpolation within the space provides an estimated solution at any crack shape and depth within the geometric space and at any modulus of elasticity and strain hardening exponent within the material space. The solution of interest is the J_n value as a function of ϕ around the crack perimeter, $J_n(\phi)$. For each of the 600 models in the space, $J_n(\phi)$ is calculated as a function of increasing deformation increment. The state of the deformation increment can be described by either the models' far field stress, σ_n, or displacement at the crack mouth, $CMOD_n$. Though σ_n (or force) is an intuitive descriptor of the load increment, for elastic-plastic analysis, the *CMOD* is a more reliable predictor of J (J is nearly a linear function of *CMOD* in the plastic regime) [4,9, 16]; so the authors chose to use *CMOD* as the characteristic loading condition in the interpolation methodology. Figure 4 shows a plot of $J_n(\phi)$ vs. $CMOD_n$ for a solution with 30 load increments. Open symbols are placed at the $\phi = 30°$ location to help visualize the J_n vs. *CMOD* trajectory for a given ϕ location. In the solution space, the

relationship between σ_n and $CMOD_n$ is maintained, thus by dividing σ_n by the final dimensioned area, a prediction of the *P* vs. *CMOD* trace is available. This trace is particularly useful for comparison with experimental surface crack test results.

The solution space consists of 600 result data sets, each containing $J_n(\phi)$ vs. $CMOD_n$ and σ_n vs. $CMOD_n$ data. The space is structured in a four dimensional array that is most easily visualized by considering a 4x5 geometry matrix with four rows of *a/B* ratios and five columns of *a/c* ratios. Within each of the 20 geometric combinations, there exist 30 material solutions described by a 5x6 matrix of material solutions, five values of *n* and six values of E/σ_{ys}. The solution space is readily indexed by these four dimensions. For a given model result, *R*, the solution is given by the notation: R(a/B, a/c, n, E/σ_{ys}). Figure 5 shows a conceptual illustration of the R(a/B, a/c, n, E/σ_{ys}) solution space with the geometric space at the highest level and the entire material space existing at the next level repeated within each geometric combination followed by the $J_n(\phi)$ vs. $CMOD_n$ and σ_n vs. $CMOD_n$ data for each of the 600 models at the lowest level.

In general, the actual surface crack geometry and material of interest will not fall directly on an existing solution and interpolation is necessary. To interpolate to a new solution, $\bar{R}\left(a/B, a/c, n, E/\sigma_{ys}\right)$, the first step is to identify the subset of the 600 model space that will be active in the interpolation process by determining the location of $\bar{R}$ in the geometry and material matrices. For illustration, consider a choice of $\bar{R}\left(a/B = 0.5, a/c = 0.5, n = 8, E/\sigma_{ys} = 400\right)$ that is located between the cells labeled g_1 through g_4 in the geometry matrix of Figure 5. The four "nearest-neighbor" subset solutions are the geometry combinations designated as $g_1 - g_4$. For each of the $g_1 - g_4$ geometries, a point for $\bar{R}$ can be placed in the material matrix resulting in

materials m_1 through m_4. Identifying the sets $g_1 - g_4$ and their associated $m_1 - m_4$ sets, provides the 16 nearest-neighbor data sets for use in the interpolation of the $\bar{R}$ solution.

Solution Verification

The surface crack solutions and the interpolation method were verified through several techniques, summarized as follows. The linear-elastic *J*-integral solutions were shown to be in proper agreement with the Newman-Raju [10,11] solutions. Domain convergence for the elastic-plastic *J*-integral values at the final load step was demonstrated for the complete set of solutions at all crack perimeter nodal locations. Twenty-five benchmark FEMs were created purposefully exploiting gaps in the geometry and material solution matrices to test the effectiveness of the interpolation method. The interpolated solutions were able to predict the benchmark *J*-integral and reaction force solutions for a given CMOD value to within a few percent. Significant effort was expended to ensure the reliability of this new tool, and the details of the verification methods are discussed in detail in NASA/TP-2013-217480 [14]

Graphical User Interface Tool

After the verification was complete, the solution space and interpolation methods were incorporated into a Matlab graphical user interface (GUI) tool as shown in Figure 6. For a set of solutions of this magnitude, a convenient and easy-to-use computer program must be created to enable ready access to the solutions. The GUI tool provides an interface for a non-expert to quickly interpolate to a fully elastic-plastic solution for a surface crack in tension. The only required inputs are the surface crack dimensions ($2c$ and a), plate cross-section dimensions (W and B), and LPPL material properties (E, σ_{ys}, and n). With the geometry and material parameters entered, the tool interpolates to the appropriate $J(\phi)$ vs. *CMOD* and σ vs. *CMOD* solution, providing the full solution as CMOD ranges from zero out to the CMOD limit of the solution

space at the given input parameters. With surface crack test design and analysis in mind, the tool also has several other useful features such as:

1. material property import capability with automated material constant fitting,
2. pre-test prediction capabilities based on a critical *J*-integral value and critical ϕ location,
3. test record *P* vs. *CMOD* evaluation and comparison with analysis,
4. the ability to review result plots such as $J(\phi)$, *J* vs. *CMOD*, and deformation limit comparisons, and,
5. the ability to save the solution and plot files.

Consolidation of these new elastic-plastic surface crack solutions and the corresponding interpolation methodology into an easily accessible program represents a significant bridge for the practicing engineer toward commonplace elastic-plastic assessment of surface crack tests.

Interpolated Solution of the Round Robin Surface Crack Test

The GUI tool was used to create an interpolated solution to compare with the author-led inter-laboratory round robin (RR) concerning the elastic-plastic analysis of surface cracked plates as documented in NASA/TM-2012-217456 [9]. A surface crack tension test was performed to serve as the basis for the RR work. The experiment existed of a 2219-T8 aluminum specimen with W = 88.82 mm, B = 9.50 mm, L = 177.8 mm (uniform cross-section length), a = 6.17 mm, and $2c$ = 12.70 mm as shown in Figure 7. The specimen was loaded under displacement control in tension until ductile tearing was detected. The tearing force was 252 kN corresponding to a tearing *CMOD* of 0.114 mm, and the location of maximum tearing along the

crack front was at $\phi = 17°$. The round robin participants were requested to blindly predict the force versus *CMOD* trace and to provide *J* versus ϕ at forces of 200, 252, and 289 kN.

The interpolated solution is compared to the FE analyses of the other fourteen RR participants. In the following section the authors' original FE analysis performed for the RR is labeled "FEA," and the other participants' results are labeled "Labs 2-15." A LPPL approximation of the material's stress-strain curve is required to estimate an interpolated solution to the problem. The interpolated solutions assume the same elastic properties provided to the RR participants ($E = 74.46$ GPa and $\nu = 0.33$) with the exception that ν is a fixed value of 0.30 in all the interpolated solutions. The authors conducted a study on the sensitivity of the interpolated solution to the choice of σ_{ys} and n, and determined that the interpolated solution is fairly insensitive to reasonable choices of flow properties [14]. Values of $\sigma_{ys} = 365.4$ MPa and $n = 9.5$ were chosen as representative of an "average" choice for material flow properties and were used to solve for the interpolated result shown here.

Figure 8 shows the comparison of the *P* versus *CMOD* test data with the authors original FEA, the interpolated solution, and the analysis results of other RR participants, labs 2-15. The interpolated solution falls directly within the family of the RR results. It is important to recall that the interpolated solution is generic, so the final *CMOD* of the *Int 3* solution is *not* part of the prediction; rather, it is the *P* versus *CMOD* trace up through any specified *CMOD* value of interest. Figure 9 compares the *J*-integral values at $\phi = 17°$ versus the *CMOD* results the interpolated solution and all of the lab solutions. Again the interpolated solution is in excellent agreement with the family of solutions represented in the round robin. It is clear from the trace of the interpolated solution that it passes cleanly through the family of RR results and provides

an answer of equivalent quality as may be expected from a custom finite element assessment of the test.

Conclusions

This paper presents a case for moving beyond equation-based test standards for certain classes of complicated fracture mechanics tests. Using automated and standardized computer tools to calculate the pertinent test result values has several advantages such as:

1. allowing high-fidelity solutions to complex nonlinear phenomena that would be impractical to express in written equation form,
2. eliminating errors associated with the interpretation and programing of analysis procedures from the text of test standards,
3. lessening the need for expertise in the areas of solid mechanics, fracture mechanics, numerical methods, and/or finite element modeling, to achieve sound results,
4. and providing one computer tool and/or one set of solutions for all users for a more "standardized" answer.

In summary, this approach allows a non-expert with rudimentary training to get the best practical solution based on the latest understanding with minimum difficulty.

As a practical example, the authors presented an automated method to determine the elastic-plastic solution for a surface crack plate in tension using interpolation methodologies. This new set of elastic-plastic surface crack solutions, the interpolation methodology, and the simple GUI implementation represents a significant step toward commonplace assessment of surface cracks by the J-integral. This is particularly true for the case of standardized experimental evaluation of surface crack fracture toughness. Unfortunately, the use of elastic-plastic experimental methods

in the evaluation of fracture toughness of materials continues to lag significantly behind linear-elastic methods, even for common two-dimensional geometries such as the compact tension specimen, despite the advantages in flexibility and breadth of information elastic-plastic methods reveal. Surface crack toughness testing can provide the most direct measure of material performance in structurally representative configurations; yet, the detailed working knowledge of finite element modeling currently required to properly assess a surface crack test in the elastic-plastic regime (as most are) has kept surface crack toughness testing reserved mainly as a domain for the specialist. The costs in modeling time and software infrastructure are largely prohibitive for most experimental labs. The interpolation methodology and solution space described herein represents a new evolutional step in tools for the analyst and experimentalist alike.

A strong case can be made for developing automated analysis tools for certain classes of complicated fracture testing standards and for providing standard computer tools as a companion with the ASTM standards. This is a novel concept in the ASTM fracture testing arena, but standard computer programs are already being used with other ASTM standards that cover complicated physical phenomena or processes such as: ASTM C1340/C1340M-10 - Standard Practice for Estimation of Heat Gain or Loss Through Ceilings Under Attics Containing Radiant Barriers by Use of a Computer Program, ASTM F 2815 - Standard Practice for Chemical Permeation through Protective Clothing Materials: Testing Data Analysis by Use of a Computer Program, and ASTM E2807 - Standard Specification for 3D Imaging Data Exchange, Version 1.0 [17-19]. The verification, validation, and round-robin processes required of a computer tool closely parallel the methods that are used to ensure the solution validity for equations included in test standards. In many ways an automated solution method using a computer program can be

thought of as a complicated equation that cannot be simply written down on a page; instead the answer has to be obtained through the use of automated numerical methods. For the surface crack example presented here, the automated interpolation method has the advantage of being a bounded problem with verified solutions that populate the space.

Of course providing a standard computer tool with an ASTM standard requires consideration of some technical details. As with any analytical method, users have to input appropriate analysis values to get reasonable solutions. Most gross input errors can be mitigated or detected by analysis comparison back to the actual test data such as the force versus *CMOD* data for the surface crack test. For any test standard incorporating automated analysis tools, the governing task group has to be willing to create the solutions and build the analytical tools to make the solutions useable and accessible. Computer tools also require consideration of details concerning configuration control, tool publishing, platform releases, and file sharing. None of these obstacles are insurmountable, and the advantages of automated analysis tools easily outweigh any difficulties.

As more complicated fracture toughness tests are considered for standardization, automated analysis tools provide a viable option for obtaining test results. The use of automated analysis tools allows the creation and practical implementation of advanced fracture mechanics test standards that capture the physics of a nonlinear fracture mechanics problem without adding undue burden or expense to the user. Providing ASTM fracture testing standards with companion computer tools has many advantages and has already been implemented by other ASTM committees. The authors especially hope the automated analysis methods presented here will provide a useful method for advanced surface crack test analysis.

References

1. ASTM E399-09. Standard Test Method for Linear-Elastic Plane-Strain Fracture Toughness K_{IC} of Metallic Materials. *Annual Book of ASTM Standards*. West Conshohocken, PA, 2012.
2. ASTM E1820-11. Standard Test Method for Measurement of Fracture Toughness. *Annual Book of ASTM Standards*. West Conshohocken, PA, 2012.
3. McClung RC, Chell GG, Lee YD, Russell DA, Orient GE. Development of a practical methodology for elastic-plastic and fully plastic fatigue crack growth. *NASA/CR-1999-209428*; 1999.
4. Anderson TL. Fracture Mechanics: Fundamentals and Applications, Third Edition. CRC Press, 2005.
5. Kumar V, German MD, Shih CF. An engineering approach for elastic-plastic fracture analysis. *Report NP-1931, Electric Power Research Institute*; 1981.
6. Kumar V, German MD, Wilkening WW, Andrews WR, deLorenzi HG, Mowbray DF. Advances in Elastic-Plastic Fracture Analysis. *Report NP-3607, Electric Power Research Institute*; 1984.
7. Kumar V, German MD. Elastic-Plastic Fracture Analysis of Through-Wall and Surface Flaws in Cylinders. *Report NP-5596, Electric Power Research Institute*; 1988.
8. Ainsworth RA. The assessment of defects in structures of strain hardening material. Engineering Fracture Mechanics. 1984; 19:633-642.
9. Wells DN, Allen PA. *Analytical Round Robin for Elastic-Plastic Analysis of Surface Cracked Plates: Phase I Results*: NASA MSFC; 2012. NASA/TM-2012-217456.
10. Newman JC, Raju IS. Stress-intensity Factor Equations for Cracks in Three-Dimensional Finite Bodies Subjected to Tension and Bending Loads. *Computational Methods in the Mechanics of Fracture*. 1986;2:311-334.
11. Newman JC, Reuter WG, Aveline CRJ. Stress and Fracture Analyses of Semi-Elliptical Surface Cracks. *ASTM Special Technical Publication*. 2000;STP1360:403-423.
12. FEA-Crack. Quest Integrity Group. http://www.questintegrity.com/products/feacrack-3D-crack-mesh-software/. Verified Dec. 12, 2012.
13. ABAQUS CAE. Dassault Systemes. http://www.3ds.com/products/simulia/portfolio/abaqus/abaqus-portfolio/abaquscae/. Verified Jan 16, 2013.
14. Allen PA, Wells DN. *Elastic-Plastic J-Integral Solutions for Surface Cracks in Tension Using an Interpolation Methodology*: NASA MSFC; 2013. NASA/TP-2013-217480.
15. WARP3D. Dodds RH. University of Illinois at Urbana-Champaign. http://code.google.com/p/warp3d/. Verified Dec. 12, 2012.

16. Brocks W, Scheider I. Reliable J-Values; Numerical aspects of the path-dependence of the J-integral in incremental plasticity. MP Materialprüfung 45 (2003) 264.

17. ASTM C1340/C1340M-10. Standard Practice for Estimation of Heat Gain or Loss Through Ceilings Under Attics Containing Radiant Barriers by Use of a Computer Program. *Annual Book of ASTM Standards*. West Conshohocken, PA, 2012.

18. ASTM F2815-10. Standard Practice for Chemical Permeation through Protective Clothing Materials: Testing Data Analysis by Use of a Computer Program. *Annual Book of ASTM Standards*. West Conshohocken, PA, 2012.

19. ASTM E2807-11. Standard Specification for 3D Imaging Data Exchange, Version 1.0. *Annual Book of ASTM Standards*. West Conshohocken, PA, 2012.

List of Figures

Figures

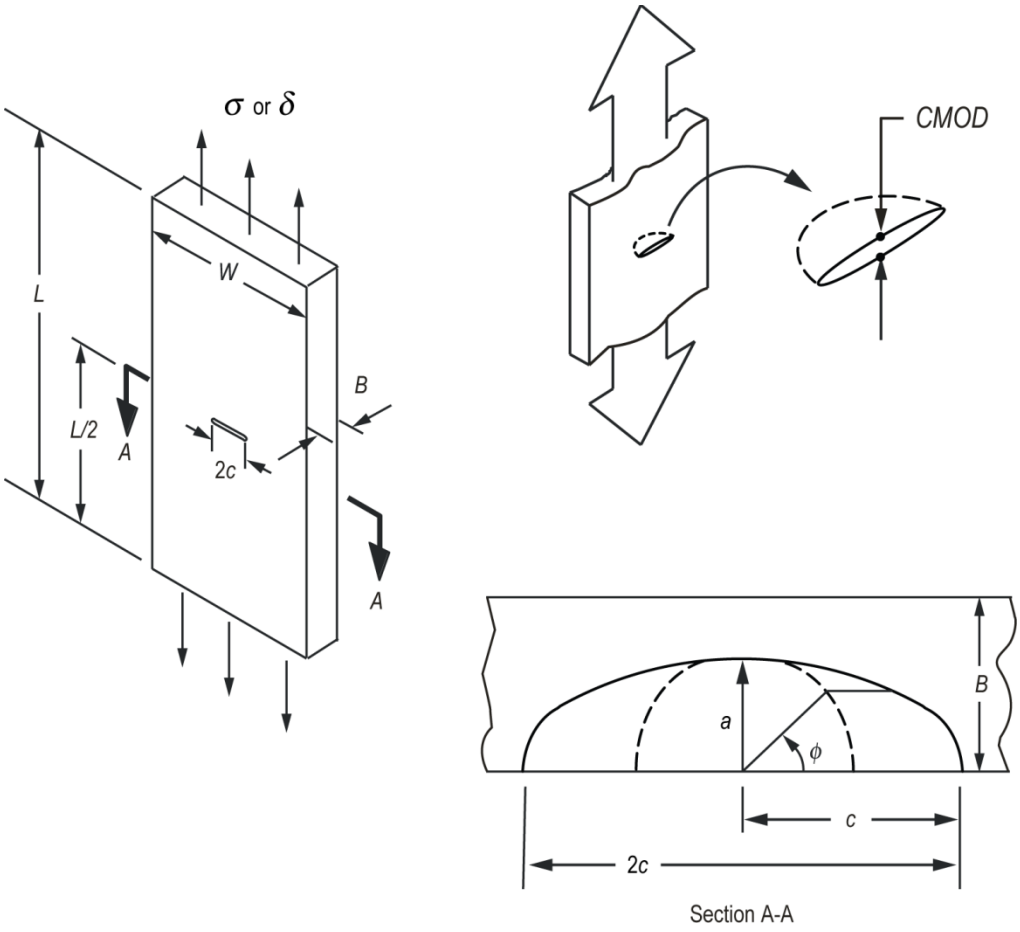

Figure 1. Illustration of a semi-elliptical surface crack in a flat plate.

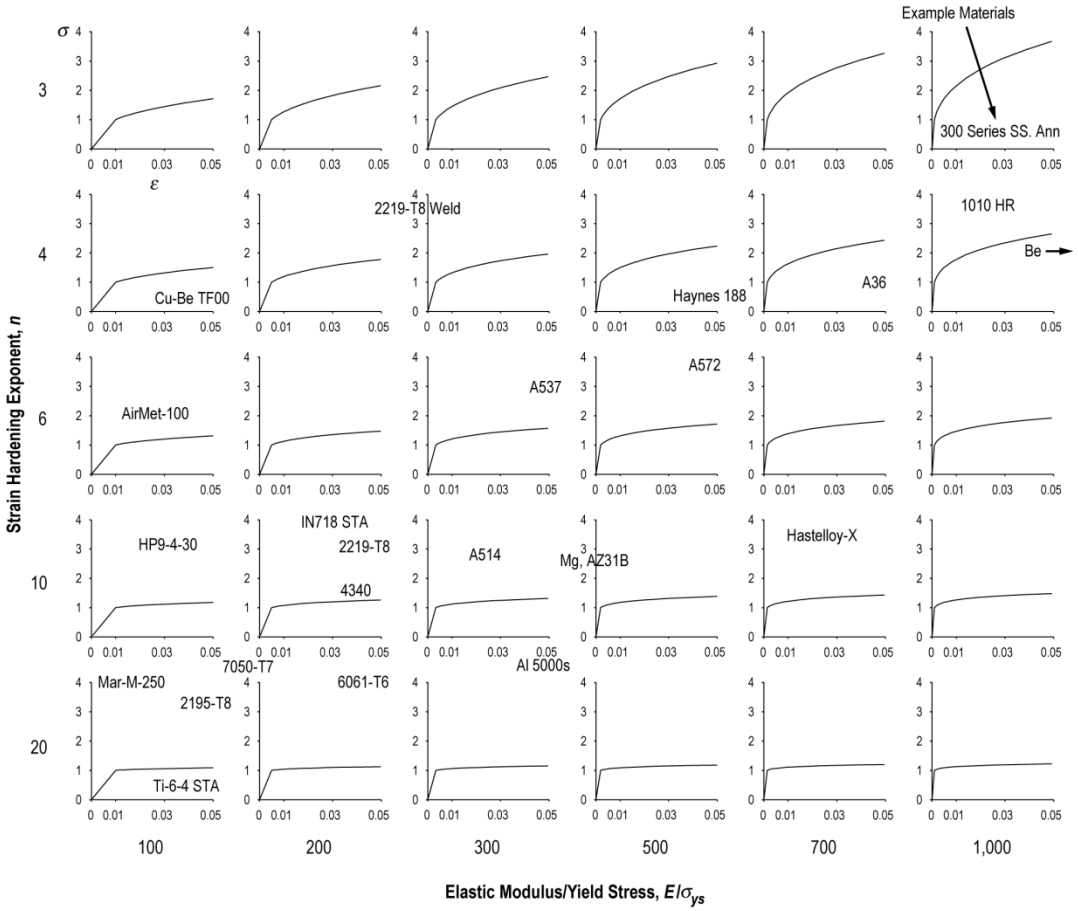

Figure 2. Illustration of the material space.

Figure 3. Illustration of the geometric space.

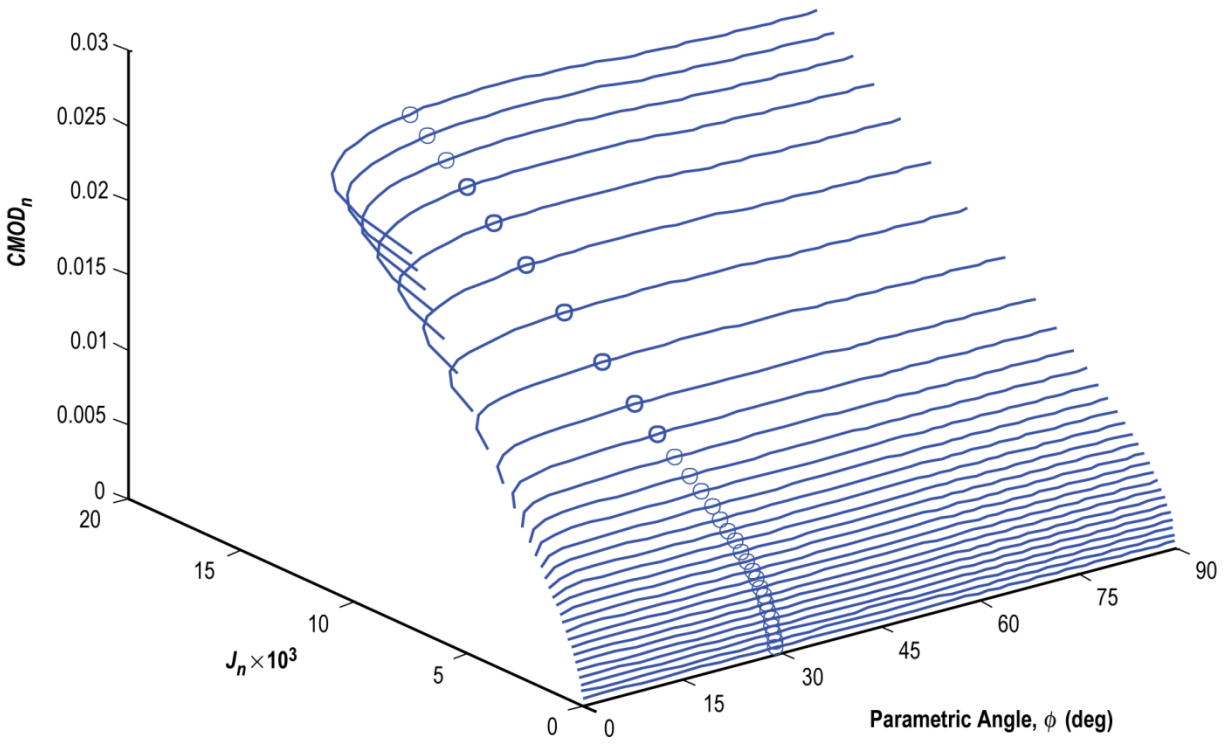

Figure 4. Example illustration of the $J(\phi)$ versus *CMOD* space.

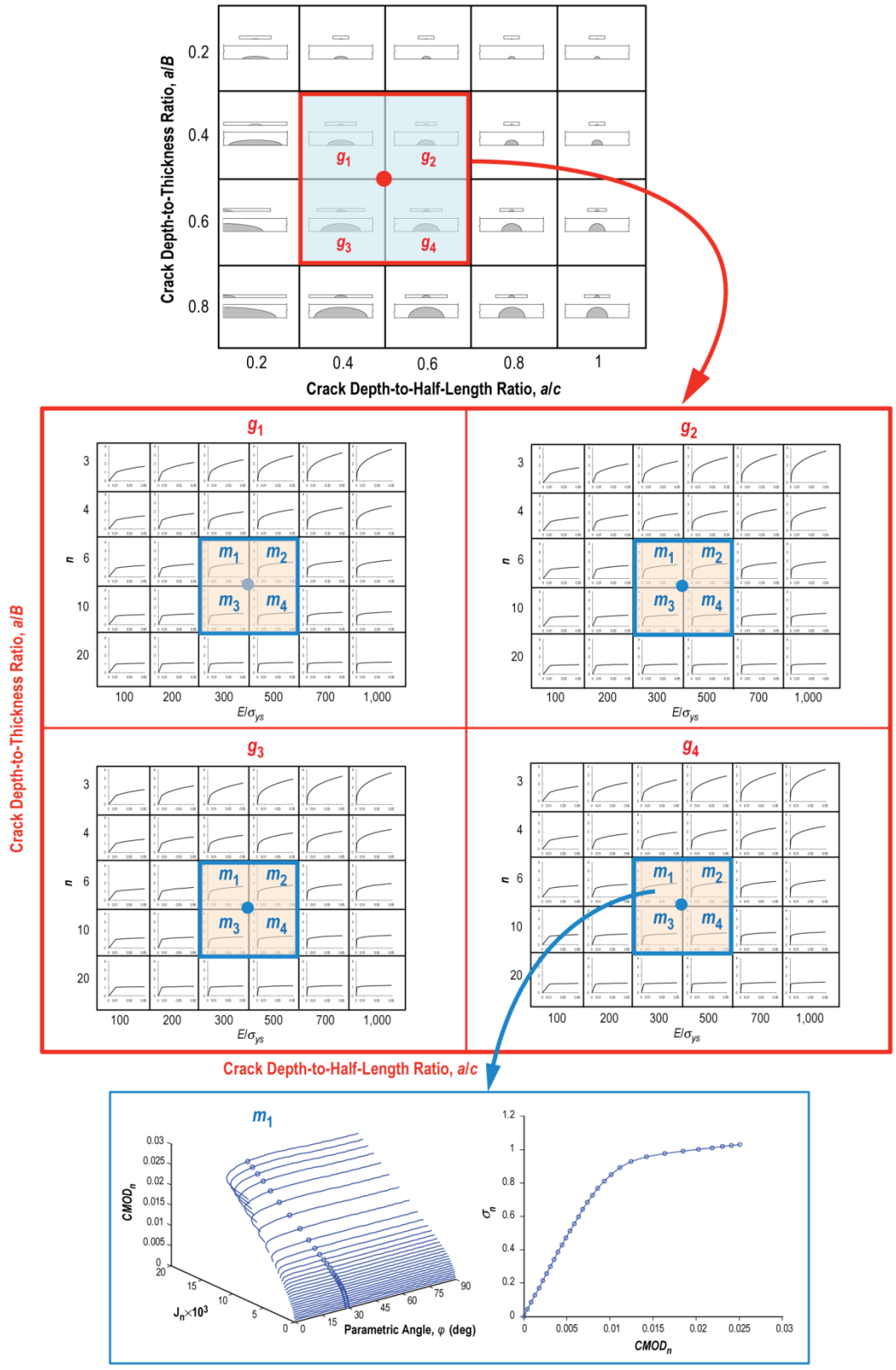

Figure 5. Conceptual illustration of the interpolation space.

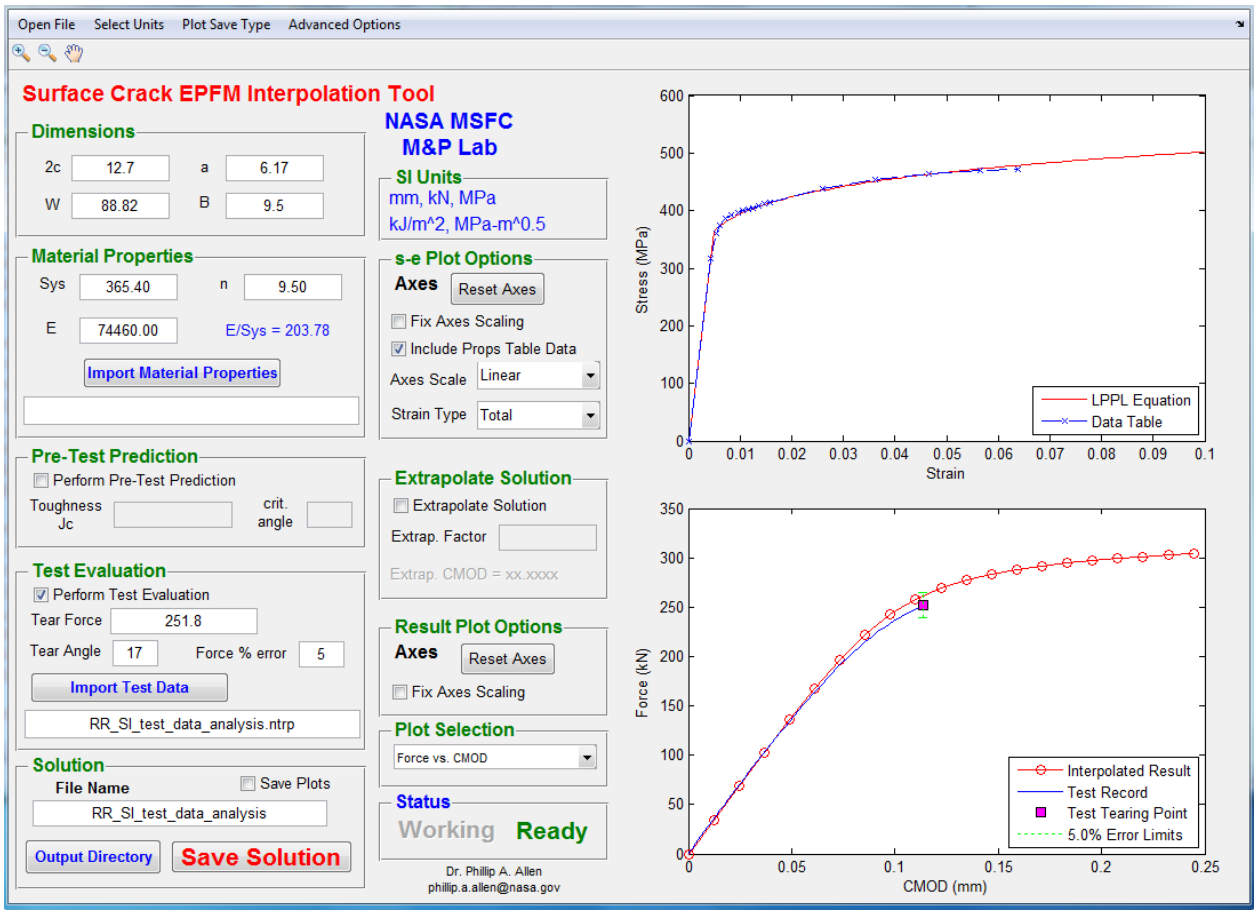

Figure 6. Computer program with GUI for automated elastic plastic surface crack analysis.

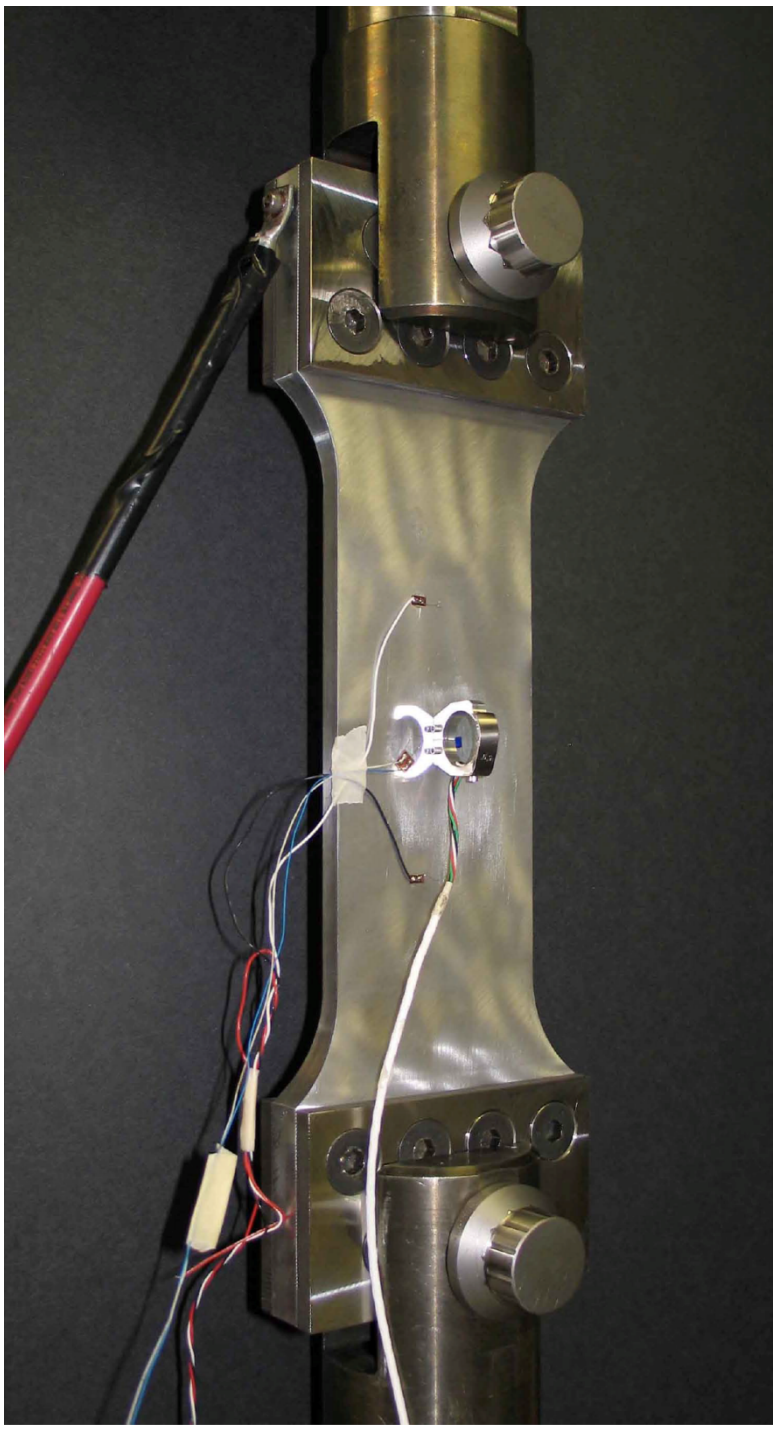

Figure 7. Round robin specimen configured for testing.

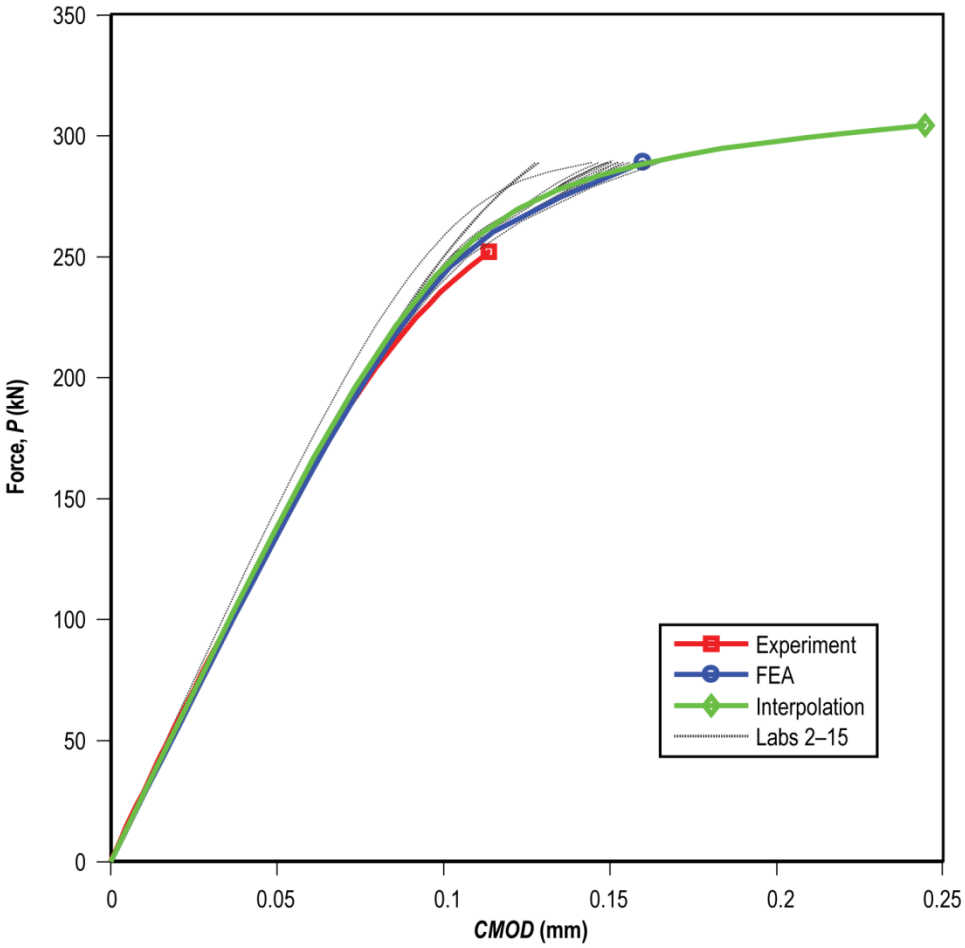

Figure 8. Interpolation, FEM , and RR participant results compared to experimental force versus *CMOD* response.

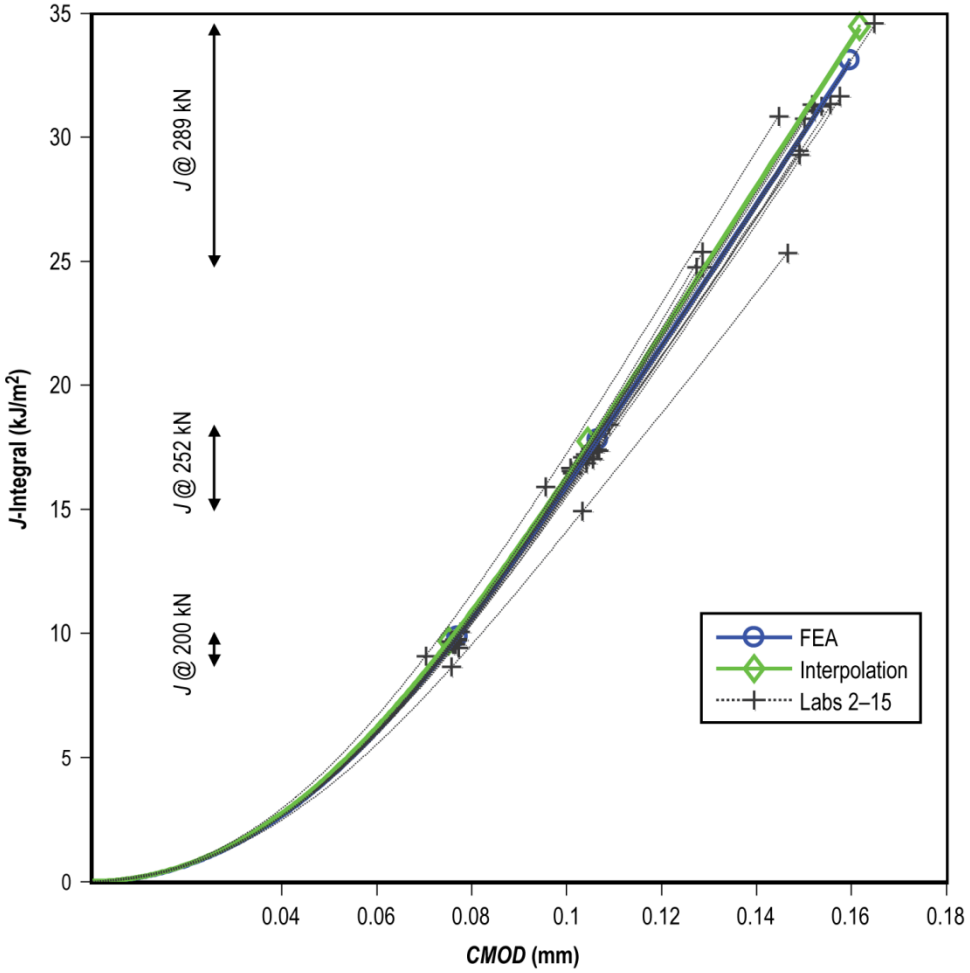

Figure 9. Comparison of interpolation, FEM, and RR participant results for $J(\phi = 17°)$ versus *CMOD*.